Chemistry and Materials Research
ISSN 2224- 3224 (Print) ISSN 2225- 0956 (Online)
Vol.7 No.3, 2015

Changes in Oil Palm Frond Fiber Morphology, Cellulose Crystallinity and Chemical Functional Groups during Cellulose Extraction Phases

Firda Aulya Syamani[1*], Subyakto[1], Sukardi[2], Ani Suryani[2]

1. Research Center for Biomaterials, Indonesian Institute of Sciences (LIPI)

Jl. Raya Bogor Km 46, West Java, 16911, Indonesia

2. Department of Agroindustrial Technology, Bogor Agricultural University

Jl. Raya Darmaga, Kampus IPB Darmaga Bogor, West Java, 16680, Indonesia

* E-mail of the corresponding author: firda.syamani@biomaterial.lipi.go.id

Abstract

Oil palm fronds (OPF) are agricultural by product and economical natural fibers resources. Cellulose is the main constituent in plant cell wall and because of its mechanical properties, cellulose fibers are potential to be utilized as reinforcement in composite product. The strength of cellulose is affected by its crystalline structure. To extract cellulose from natural fibers, lignin and hemicellulose have to be separated for instance by pulping and bleaching process. The main goal of this study was to observe changes in the OPF fibers morphology, cellulose crystallinity and chemical functional groups during cellulose extraction phases. Soda pulp of OPF was bleached using hydrogen peroxide. Subsequently, the bleached pulp was reacted with potassium hydroxide to eliminate hemicellulose. Afterward, further hydrogen peroxide bleaching was conducted to extract the cellulose. Surface morphological study using SEM revealed that there was a reduction in fiber diameter during cellulose extraction. Cellulose crystallinity and chemical functional groups at each phase of cellulose extraction were slightly different as demonstrated by XRD and FTIR analysis.

Keywords: oil palm frond soda pulp, cellulose extraction, fiber morphology, cellulose crystallinity

1. Introduction

Cellulose is available by nature in abundant quantities, either from wood or non wood resources. Within wood and natural fibers, cellulose is attached in lignin matrix and associated with hemicellulose, so that is often referred to as the lignocellulosic materials. To extract cellulose from lignocellulosic materials, lignin and hemicellulose have to be separated for instance by pulping and bleaching process.

As a high molecular weight linear homo-polymer, cellulose has the basic molecular format of $C_6H_{10}O_5$, which is called anhydroglucose (AGU). Unit of AGU was connected each other by hydrogen bonding to form supermolecular cellulose either by intermolecular hydrogen bonding or intramolecular hydrogen bonding. In nature, cellulose polymer chain consists of crystalline region and amorphous region. Crystalline region are interrupted every 60 nm with non-crystalline amorphous regions, which were folds in cellulose polymer chain, called “defects” (De Souza *et al.* 2002). The strength of cellulose was due to its crystalline structure. Cellulose crystal structural has modulus of elasticity (MoE) of 120-140 GPa (Tashiro & Kobayashi *et al.* 1990) and induced fiber stiffness, while the bulk modulus of cellulose was measured as 20 GPa (Cabrera *et al* 2011). Cellulose modulus of elasticity depends on its crystallinity and the interaction of amorphous and crystalline region (Cabrera *et al*. 2011). Due to those mechanical characteristics, cellulose has high tensile strength and functioned as reinforcing agent in wood (lignocellulosic materials). Having high tensile strength, cellulose is also potential to be utilized as reinforcing agent in composite products.

The crystallinity index (CI) of cellulose has been examined using several different techniques including X-Ray Diffractometer (Evans *et al.* 1995; Zaibo *et al.* 2007; Gumuskaya *et al.* 2003), Fourier Transform Infra Red spectroscopy (Evans *et al*. 1995; Gumuskaya *et al*. 2003), Nuclear Magnetic Resonance (Evans *et al*. 1995; Zaibo *et al.* 2007). Among of those techniques, XRD has some advantages. X-ray diffraction measures the fraction of molecules which are arranged in a regular repeating pattern (Mann 1962) and gives more detailed data on features of crystalline, although less on the non-crystalline fraction of cellulose (Terinte *et al.* 2011). X-ray diffraction provides strong signals from crystalline fraction of the cellulose. These signals can be used to determine crystallographic parameters, like measuring the distances in the crystalline unit cell (Zugenmaier

2001). There are 3 methods used for calculating CI from the raw spectrographic XRD data (Park *et al*. 2010). First, CI was calculated from the height ratio between the intensity of the crystalline peak (I_{002} - I_{AM}) and total intensity (I_{002}) after subtraction of the background signal measured without cellulose (Segal *et al*. 1962). Second, individual crystalline peaks were extracted by a curve-fitting process from the diffraction intensity profiles (Hult *et al.* 2003). Third, ball-milled cellulose was used as amorphous cellulose to subtract the amorphous portion from the diffraction profiles (Thygesen *et al*. 2005). After subtracting the diffractogram of the amorphous cellulose from the diffractogram of the whole sample, the CI was calculated by dividing the remaining diffractogram area due to crystalline cellulose by the total area of the original diffractogram.

One of cellulose sources that available in huge amount in Indonesia is oil palm frond (OPF). To extract cellulose from OPF, lignin and hemicellulose have to be separated by pulping and bleaching process. The main goal of this study was to monitor changes in the fiber morphology, cellulose crystallinity and chemical functional groups during each phase of cellulose extraction from OPF fibers.

2. Materials and Methods

2.1 Materials

Oil palm fronds (OPF) were obtained from oil palm plantation in West Java, Indonesia. The sodium hydroxide at technical grade was used in pulping process. Bleaching process used technical grade of hydrogen peroxide. Potassium hydroxide was supplied by Merck.

2.2 Cellulose Extraction: Pulping, Bleaching and Purifying Processes

The OPF fibers were sun-dried and cut into ± 2 cm length. The moisture content of fibers was 11%. To produce soda pulp, OPF fibers were subjected to digester with ratio of liquor-to-materials was 8:1. Soda pulping was carried out at 45% alkali charge. NaOH solution with concentration of 490 g/L and water were added to digester by 410 mL and 3140 mL, respectively to cook 500 g OPF fibers (dry basis). Pulping was conducted in 2 h and 46 min, at 176°C. After cooling of the digester, the pulp was collected and washed with water several times until neutralized.

For the bleaching process, as much of 20 g pulp (dry basis) and 300 ml distilled water were added in 500 ml erlenmeyer, then put in waterbath at 80°C. The technical grade solution of 50% hydrogen peroxide was used as bleaching agent. Every 60 min, 8 ml of 50% hydrogen hydroxide was added into erlenmeyer, for 3 times. After 4 h bleaching process, bleached pulp was collected and washed with running water.

In order to eliminate hemicellulose content, bleached pulp were reacted with 5% (w/v) potassium hydroxide in waterbath at 80°C for 2 h, followed by washing with running water. The final stage to produce cellulose was further bleaching process with 8 ml of 50% hydrogen peroxide for an hour at 80°C.

2.3 Charaterization of Cellulose by Scanning Electron Microscope

The morphological of OPF soda pulp, bleached pulp, purified pulp and cellulose were analyzed by scanning electron microscope/energy dispersive spectroscope (SEM/EDS) ZEISS EVO 50, operated at 10 kV. Samples were coated with gold using a vacuum sputter-coater to improve conductivity of the samples and thus the quality of the SEM images.

2.4 Charaterization of Cellulose by X-Ray Diffractometer

XRD measurements were performed on a Shimadzu XRD7000 MAXima X-ray diffractometer equipped with computerized data collection and analytical tools to analyze cellulose crystallinity. The diffracted intensity of Cu Kα radiation (λ= 1.54 Å; 40.0 kV and 30.0 mA) was measured in a 2θ range between 10° and 40° with scan speed of 2.0 deg/min.

To determine cellulose degree of crystallinity, we used built-in degree of crystalization software to separate amorphous and crystalline contribution to the diffraction spectrum using a curve-fitting process of Lorentzian function. Degree of crystallinity is calculated from the ratio of the area of all crystalline peaks to the total area.

The average size of crystallite (Gumuskaya *et al*. 2003) was calculated from the Scherrer equation (Eq. 1). This is a method based on the width of the diffraction pattern in the X-ray reflected crystalline region. In this study, the crystallites size were determined by using diffraction pattern obtaining from 101, 10-1, 002 and 040 lattice planes of samples.

$$D = \frac{k\lambda}{B\cos\theta} \quad (1)$$

where D is the crystallite size (in nm), k is the Scherrer constant (0.84), λ is x-ray wavelength (0.154 nm), B is the FWHM (full width at half maximum) of peak diffraction (in rad), θ is the corresponding Bragg angle.

2.5 Charaterization of Cellulose by Fourier Transform Infra Red Microscope

The ABB FT IR MB3000 was used to analyze chemical structure of OPF pulp component. The analysis was run using the KBr pellet technique. The KBr pellets of samples were prepared by mixing 2 ±0.05 mg of pulp sample with 200 mg KBr (spectroscopy grade) in a vibratory ball mixer for 20 s. The KBr pellets were prepared under vacuum in a standard device under a pressure 80 KN.cm^{-2} for 3 min to form pellet with diameter and thickness of 13 mm and 0.5 cm, respectively. The spectral resolution was 4 cm^{-1} and the scanning range was from 400 to 4000 cm^{-1}.

3. Results and Discussion

Cellulose was extracted from OPF fibers in 4 phases: pulping, bleaching, purifying and second bleaching. We studied cellulose morphology, crystallinity and functional groups in every phase.

3.1 Morphology of Oil Palm Frond Fiber

Scanning electron microscope (SEM) images of OPF fiber are demonstrated in Fig. 1. OPF fiber contained various sizes of vascular bundles. The vascular bundles were widely imbedded in thin-walled parenchymatous ground tissue. Each bundle was made up of a fibrous sheath, vessels, fibers, phloem and parenchymatous tissues. Xylem and phloem tissues are clearly distinguishable. Phloem was divided into two separate areas in each bundle. Some vascular bundles also contained several well-defined proto-xylem elements. Proto-xylem and meta-xylem vessels in the bundle were separated by a layer of parenchyma cells (Abdul Khalil *et al*. 2006).

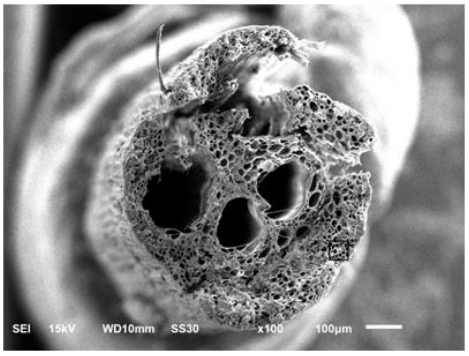

Figure 1. Oil palm frond fiber (OPF) morphology at 100x magnifications

3.2 Morphology characteristics of OPF soda pulp, bleached pulp, purified pulp and cellulose fibers

Scanning electron microscope (SEM) images of OPF soda pulp, bleached soda pulp, purified pulp and cellulose fibers are demonstrated in Fig. 2. After undergo bleaching and purifying process, OPF fibers tend to split in longitudinal direction and formed a flatten fibers. Some fibers still remain in quite compact structure. While some others were flatten resulting flat fibers.

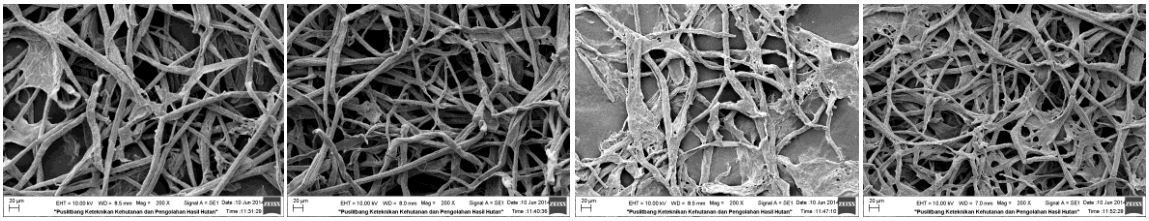

Figure 2. SEM images of (a) soda pulp, (b) bleached pulp, (c) purified pulp and (d) cellulose fibers of OPF

During bleaching, hydrogen peroxide removed residual lignin and reacted with non-lignocellulosic components. These reactions produced some materials that observed at the background of fibers (Fig. 2b). To obtain purified pulp, bleached pulp was reacted with potassium hydroxide. It appears that hemicellulose was separated from

fibers then reacted with non-lignocellulosic components and materials at the background of fibers become more obvious (Fig 2c).

Observation at 2500x magnification showed that the disruption of structure OPF cellulose (Fig. 3). The pulping processed at 176°C for 2 hr and 46 min, purifying and further bleaching processes lead to cause the defect of cellulose fiber's surface.

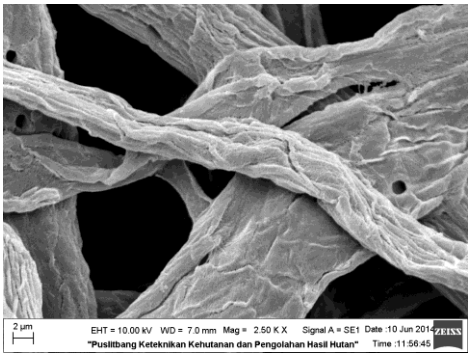

Figure 3. SEM image of cellulose fibers of OPF (2500x mag)

The inorganic constituents of OPF soda pulp, bleached pulp, purified pulp and cellulose were also studied by energy dispersive X-ray analysis. Table 1 shows the energy dispersive X-ray analysis (SEM-EDX) with the elemental composition of OPF. No specific difference was demostrated between the four samples. The specimens had carbon and oxygen in a large weight percentage, while little of the zinc, tungsten, platinum, copper, calcium, and magnesium existed in oxide form.

Oxygen was observed in a significant quantity in bleached pulp. During bleaching process, soda pulp was reacted with hydrogen peroxide and the bleaching action of hydrogen peroxide was the chemical oxidation of chromophore by the perhydroxyl anion.

Table 1. Inorganics constituents in soda pulp, bleached pulp, purified pulp and cellulose of OPF

Element	Norm. C [wt.%]			
	Soda Pulp	Bleached Pulp	Purified Pulp	Cellulose Fibers
Carbon	45.01	41.00	46.77	47.68
Oxygen	34.92	44.14	38.71	33.56
Zinc	5.60	3.70	2.57	4.88
Tungsten	6.08	4.17	4.31	6.15
Copper	8.36	5.13	5.58	6.22
Calcium		1.02	0.66	0.91
Magnesium		0.85	1.38	0.60

Hydrogen peroxide is one of the most widely used oxygen-based bleaching chemical in the pulp and paper industry (Ziaie-Shirkolaee 2009). In alkaline media, equilibrium of H_2O_2 shifts to the formation of perhydroxyl anion (^{-}OOH) and the ionic oxidant is used as a lignin-degrading agent in pulp bleaching (Ziaie-Shirkolaee 2009). However, during alkali hydrogen peroxide bleaching, the degree of carbohydrate degradation is essentially controlled by the concentration of active radical species (hydroxyl and super oxide anion radicals) originated from peroxide decomposition under alkaline conditions in the presence of transition metals such as Fe, Cu and Mn (Shatalov & Pereira 2005). Fortunately, the present of magnesium ion (Mg^{2+}), calcium ion (Ca^{2+}) and $SiO3^{2-}$ can slow the rate of reaction between hydroxyl radicals and carbohydrate structure (Potucek & Milichovsky 2000).

3.3 Cellulose crystallinity of OPF soda pulp, bleached pulp, purified pulp and cellulose fibers

X-ray diffraction analysis was conducted to determine the cellulose-crystallinity-degree of OPF soda pulp, bleached pulp, purified pulp and cellulose fibers. X-ray diffraction provides strong signals from the crystalline fraction of the cellulose. The cellulose-crystallinity-degree measurement by X-ray diffraction deconvolution method (Terinte *et al.* 2011) was described as follow. A technique using deconvolution procedures is applied for crystallinity measurements using suitable software to separate the non-crystalline and crystalline contributions to the diffraction spectra. For the curve fitting method, linear backgrounds were fitted to a simulated profile, based

on the convolution of sharp peaks and one broad peak representing the non-crystalline reflection. The non-crystalline part of the cellulose structure is represented by broader and less clearly refined features in the diffraction pattern. This leads to challenges in the evaluation of the signals for a quantitative crystallinity measurement.

The X-ray diffractogram of OPF soda pulp shows a quite different pattern with the four peaks characteristic of native cellulose (cellulose Iβ). Oudiani *et al*. (2011) proposed that the diffraction peaks for cellulose I from *Agave americana* L. fiber were located at 2θ = 14°, 16°, 23° and 35°, which are the positions of the (101), (10-1), (002) and (040), respectively. Whereas the diffraction peaks for cellulose II were located at 2θ = 11°, 20°, 22° and 37°. In this study, the peaks of X-ray signals from OPF soda pulp, bleached pulp, purified pulp and cellulose demonstrate the pattern of cellulose I (peaks at 2θ = 15°, 16°) and cellulose II (peaks at 2θ = 20°, 22°), as shown in Table 2 and Figure 4. Pulping with NaOH at 45% alkali charge and 176°C for 2 h and 46 min caused alteration of some portion of cellulose I into cellulose II.

Tabel 2. X ray diffraction peaks from sampels OPF

Samples	2θ angle of lattice plane (°)						d spacing (nm)						FWHM (degree)					
	101	10-1	021	002	-122	040	101	10-1	021	002	-122	040	101	10-1	021	002	-122	040
Soda pulp	15.0	15.7	20.7	22.5	29.4	34.2	0.589	0.565	0.428	0.395	0.304	0.262	1.360	2.680	1.080	1.640	0.540	0.853
Bleached pulp	15.6	16.2	20.7	22.5	29.4	34.4	0.567	0.547	0.429	0.394	0.304	0.260	2.320	1.760	1.160	1.587	0.510	1.190
Purified pulp	15.4	16.5	20.8	22.4	29.3	34.3	0.573	0.537	0.427	0.396	0.305	0.261	2.320	1.080	1.253	1.610	0.550	1.220
Cellulose	15.4	16.2	20.6	22.4	29.3	34.3	0.574	0.547	0.431	0.396	0.305	0.261	2.040	1.500	1.200	1.607	0.620	1.470

The observed cellulose I allomorph was cellulose Iβ which was a cotton-ramie type of cellulose. Wada *et al*. (2001) has accomplished to estimate ratio of cellulose Iα/Iβ from the two equatorial d-spacings of crystal using discriminant analysis. The function used to discriminate between cellulose Iα and Iβ is presented as: Z = 1693d1 – 902d2 – 549, where Z>0 indicates the algal-bacterials (Iα-rich) type and Z<0 indicates the cotton-ramie (Iβ dominant) type. In this study, d-spacings of crystal at lattice plane 101 and 10-1 were defined as d1 and d2, respectively.

OPF soda pulp, bleached pulp, purified pulp and cellulose fibers indicated crystallinity of 59.83%, 53.94%, 59.50% and 57.19%, respectively. The crystallinity of OPF soda pulp was higher than that of OPF bleached pulp crystallinity. It was not common. Because, the purpose of bleaching with hydrogen peroxide was to degrade lignin in soda pulp, through chemical oxidation of chromophore by the perhydroxyl anion from hydrogen peroxide decomposition. It appears that copper ion which was exist more than magnesium ion or calcium ion in OPF soda pulp caused the failure of bleaching agent to degrade lignin and tend to degrade carbohydrate instead.

The subsequent process when bleached pulp was reacted by potassium hydroxide at the purifying phase, the resulted purified pulp had higher crystallinity than bleached pulp. Potassium hydroxide was able to react with amorphous materials (hemicellulose) from bleached pulp then increased the pulp crystallinity. According to Lindedahl (2008), alkali in the cooking liquor is basically consumed in three different reactions: 1. with lignin, 2. neutralization of organic acids, 3. with resins in the wood. Most of the alkaline is consumed in the cooking process by the saccharine acids formed in the degradation of hemicelluloses.

However the purified pulp has darker color than bleached pulp. We assumed, it was caused by the reaction between potassium hydroxide with residual lignin. To obtain cellulose with brighter color, we conducted second bleaching process using hydrogen peroxide and it was successful to increase the crystallinity and to produce brighter color cellulose. Although we can obtain cellulose fiber with brighter color, the crystallinity was slightly reduced. This phenomenon was due to the existing of copper ion obstruct the chemical oxidation of chromophore by the perhydroxyl anion.

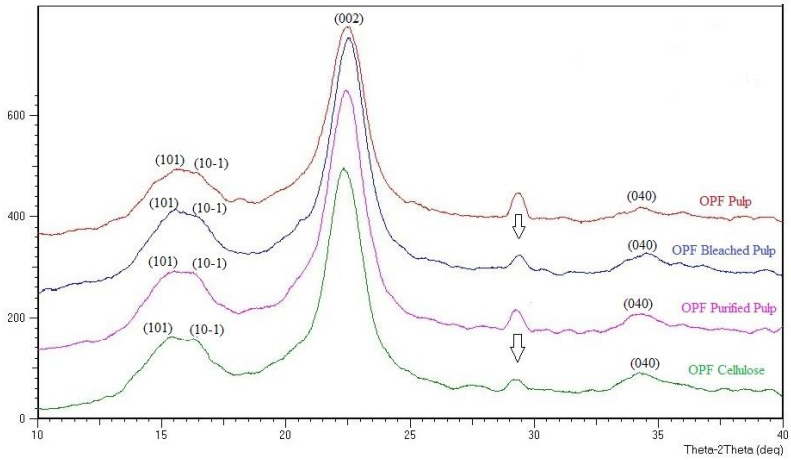

Figure 4. XRD diffractograms of OPF (a) soda pulp, (b) bleached pulp, (c) purified pulp and (d) cellulose

In addition for measuring cellulose crystallinity, x- ray diffraction signals can be used to determine crystallographic parameters, like measuring the distances in the crystalline unit cell (Zugenmaier 2001) or crystallite size (Nishiyama *et al*. 2000). Crystallite size of cellulose in pulp samples (Table 3) was determined by using the diffraction pattern obtained from 101, 10-1, 002 and 040 lattice planes. The strongest intensity, from the (002) plane, occur at the Bragg angle of 22.5° for soda pulp and bleached pulp and at Bragg angle of 22.4° for purified pulp and cellulose. However it was not correspond to the largest of crystallite size. According to Evans *et al.* (1995), the width of the peak in the diffractogram are inversely proportional to the lateral width of the crystallites. For a constant fraction of crystalline structure, as the crystallite get smaller, the crystalline "peaks" get broader and the "amorphous" background increases until eventually they become indistinguishable.

Table 3. Degree of crystallinity and crystallite size of OPF pulp and cellulose

Samples	Degree of crystallinity (Xc)			Crystallite Size (nm)			
	Crystalline (Fc)	Amorphous (Fa)	Xc (%)	D(101)	D (10-1)	D (002)	D (040)
Soda pulp	1.141	0.766	59.83	11.00	5.59	9.22	18.18
Bleached pulp	1.321	1.128	53.94	6.45	8.51	9.53	13.05
Purified pulp	1.281	0.872	59.50	6.45	13.87	9.39	12.72
Cellulose	1.309	0.980	57.19	7.34	9.99	9.41	10.56

Table 3 shows the crystallite size of cellulose in OPF soda pulp, bleached pulp, purified pulp and cellulose fibers at lattice plane (101), (10-1), (002) and (040). The crystallite size of OPF cellulose at lattice plane (002) was 9.41 nm, this was similar to crystallite size of wheat straw alpha cellulose, which was 9.1 nm (Gumuskaya & Usta 2002). Furthermore, Gumuskaya found that crystallite size of cellulose in unbleached soda pulp, hypochlorite bleached pulp, peroxide bleached pulp of wheat straw were 3.4, 4.3 and 4.6 nm, respectively. In this study, there was no significant difference in crystallite size of celluloses from OPF sampels at different phases of cellulose extraction. Cellulose extraction phases (pulping, bleaching, purifying and second phase bleaching) had no significant influence in cellulose crystal structure based on observation in cellulose allomorph, cellulose crystallinity and cellulose crystallite size. OPF pulping process with 45% alkali charge, in 2 h and 46 min, and temperature at 176°C, has already successed to eliminate lignin and hemicellulose and extract cellulose effectively.

3.4 Functional groups of OPF soda pulp, bleached pulp, purified pulp and cellulose

FTIR spectroscopy was utilized as an analytical tool for qualitatively determine the chemical changes in the surface of OPF soda pulp, bleached pulp, purified pulp and cellulose to complement and understand the XRD investigations. The infrared spectra in the 400-4000 cm^{-1} region were shown in Fig.5. The cellulose extraction process of OPF only effected the changes in band intensity without changes in functional groups (Table 4). A strong and broad hydrogen bonded (O-H) streching absorption was seen at 3348 cm^{-1} (peak 1) and a prominent

C-H streching absorption was seen at around 2901 cm^{-1} (peak 2) (Oh *et al*. 2005). In the finger print regions between 1750 ~ 800 cm^{-1}, the defined peaks were found. The peaks in this region were 1643 cm^{-1} (peak 3) for carbonyl band (Bodirlu & Teaca 2009), 1427 cm^{-1} (peak 4), 1373 cm^{-1} (peak 5) and 1319 cm^{-1} (peak 6) for CH_2 bending, CH bending and CH_2 wagging motion in cellulose (Oh *et al*. 2005). The peaks at 1242 cm^{-1} (peak 7), 1165 cm^{-1} (peak 8), 1111 cm^{-1} (peak 9), 1057 cm^{-1} (peak 10) and 895 cm^{-1} (peak 11) were assigned to strong CO streching in cellulose (Bodirlau & Teaca 2009), COC asymetric bridge oxygen streching in cellulose and hemicellulose, aromatic skeletal and CO streching in cellulose, CO streching in cellulose and hemicellulose, COC streching at the β-(1-4) glycocidic linkage, respectively (Oh *et al*. 2005).

After pulping, delignification of OPF fibers was observed in FTIR spectra. There was no signal of lignin due to no signal in region between 1465 ~ 1595 cm^{-1}. According to Lionetto, signals FTIR spectra for lignin observed at 1463 cm^{-1}, 1512 cm^{-1}, 1595 cm^{-1} and 1269 cm^{-1} that were assigned for asymmetric bending in CH_3, C=C streching of aromatic ring and CO streching in lignin (Lionetto *et al*. 2012). In addition, the presence of functional groups such as methoxyl -O-CH_3, C-O-C and aromatic C=C, peaks in the region between 1830 cm^{-1} and 1730 cm^{-1} were also not observed. The peak presents at 1730-1740 cm^{-1} in FTIR the spectra are corresponding to the presence of C=O lingkage, which are the characteristics of lignin groups (Owen & Thomas 1989). Soda pulping has succesfully delignified OPF fibers. Lignin has been recognized as amorphous component in lignocellulosic material and considered to influence crystallinity of bleached pulp, purified pulp and finally cellulose of OPF.

Table 4. Band characteristics of FTIR spectra

Wavenumber (cm-1) / absorbance height(abs)				Assignment	Related to	References
Soda Pulp	Bleached Pulp	Purified Pulp	Cellulose			
3348 / 0.55	3348 / 0.91	3348 / 0.74	3348 / 0.72	Streching(γ) OH (hydrogen bond)	cellulose	[23]
2901 / 0.23	2901 / 0.39	2901 / 0.31	2901 / 0.31	γCH		[23]
1643 / 0.19	1643 / 0.27	1643 / 0.22	1643 / 022	CO (carbonyl band)		[24]
1427 / 0.27	1427 / 0.45	1427 / 0.36	1427 / 0.34	Bending (δ) CH_2 (sym) at C-6	cellulose	[23]
1373 / 0.29	1373 / 046	1373 / 0.36	1373 / 0.36	δCH	cellulose	[23]
1335 / 0.27		1335 / 0.34		δCOH in plane at C-2 or C-3	cellulose	[23]
1327 / 0.26				γCH in cellulose	cellulose	[27]
	1319 / 0.44	1319 / 0.34	1319 / 0.35	δCH_2 (wagging) at C-6	cellulose	[23]
	1281 / 0.33		1281 / 026	δCH	cellulose	[23]
	1242 / 0.33	1242 / 025	1242 / 0.26	γCO in ester bond		[24]
1165 / 0.42	1165 / 0.74	1165 / 0.57	1165 / 0.58	γCOC at β-glycosidic	cellulose	[23]
1111 / 0.50	1111 / 0.88	1111 / 0.70	1111 / 0.70	γring in plane	cellulose	[23]
1057 / 0.62	1057 / 1.06	1057 / 0.85	1057 / 0.84	γCO at C-3, γC-C	cellulose	[23]
895 / 0.16	895 / 0.28	895 / 0.21	895 / 0.22	γCOC at β-glycosidic, γCCH at C-5 and C-6	cellulose	[23]
663 / 0.27	663 / 0.47	663 / 0.37	663 / 0.37	δCOH out of plane	cellulose	[23]

Typical bands assigned to cellulose were located at 1427 cm^{-1} and 1373 cm^{-1} for CH_2 and CH bending mode, respectively. To distinguish between amorphous and crystallized cellullose, the bands at 1335 cm^{-1} and 1319 cm^{-1} for hydroxyl in plane bending and CH_2 wagging, respectively were observed. Then the band at 1165 cm^{-1} which associated with C-O-C asymetric bridge oxygen and the band at 895 cm^{-1} which associated with asymetric out of phase ring streching, were also assigned to cellulose (Lionetto *et al.* 2012).

The enhanced absorption band at 1165 cm^{-1} and 895 cm^{-1} (Fig. 5) were observed, assigned that the β-glycosidic in bleached pulp, purified pulp and cellulose fibers were increased in comparison with soda pulp. It means that in that sampels, more cellulose were observed due to the elimination of lignin and hemicellulose. In accordance to amorphous cellulose, the band at 1335 cm^{-1} was observed in soda pulp and purified pulp. Whereas related to crystallized cellulose, the band at 1319 cm^{-1} was observed in bleached pulp, purified pulp and cellulose fibers.

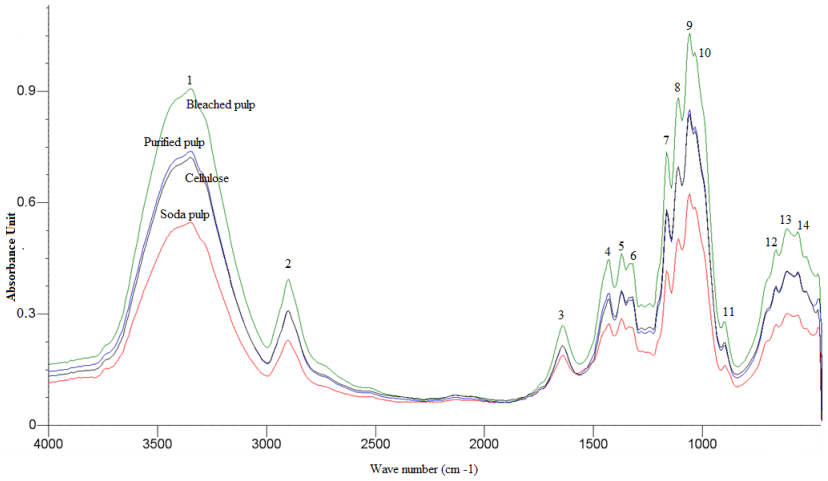

Fig 5. FTIR spectra of OPF soda pulp, bleached pulp, purified pulp and cellulose

4. Conclusion

After undergo bleaching and purifying process, OPF fibers tend to split and formed a flatten fibers. The present of copper ion in soda pulp of OPF obstruct the accomplishment of bleaching process and influenced the cellulose crystallinity in bleached pulp. Purifying process slightly increased the cellulose crystallinity of OPF pulp. The cellulose extraction process of OPF only caused the alteration of pulp component amount as demonstrated by FTIR band intensity changes. For further research, OPF cellulose fibers as form of bleached pulp can be potentially utilized as reinforcement in composite product.

Acknowledgements

This research was part of first author's dissertation and financially supported by Ministry of Research and Technology of Indonesia (Kemenristek) and Indonesia Endowment Fund for Education (LPDP).

References

Abdul Khalil H.P.S., Siti Alwani M., Mohd Omar A.K. (2006). Chemical composition, anatomy, lignin distribution and cell wall structure of Malaysian plant waste fibers. *BioResources*, **1**(2), 220-232.

Bodirlau, R., Teaca, C.A. (2009). Fourier transform infrared spectroscopy and thermal analysis of lignocellulose fillers treated with organic anhydrides. *Rom. Journ. Phys*., **54**, Nos. 1-2, 93-104.

Cabrera, R.Q., Meersman, F., McMillan, P.F., Dimitriev, V. (2011). Nanomechanical and structural properties of native cellulose under compressive stress. *Biomacromolecules*, **12**, 2178-2183.

De Souza, I.J., Bouchard, J., Methot, M., Berry, R., Argyropoulos, D.S. (2002). Carbohydrates in oxygen delignification, Part I: changes in cellulose crystallinity. *J. Pulp Paper Sci*, **28** (5), 167-170.

Emandi, A., Vasiliu, C.I., Budrugeac, P., Stamatin, I. (2011). Quantitative investigation of wood composition by integrated FT-IR and thermogravimetric methods. *Cellulose Chem. Technol*., **45** (9-10), 579-584.

Evans, R., Newman, R.H., Roick, U.C., Suckling, I.D., Wallis, A.F.A. (1995). Changes in cellulose crystallinity during kraft pulping, comparison of Infrared, X-ray Diffraction and solid state NMR results. *Holzforschung*, **45**, 498-504.

Gumuskaya, E., Usta, M. (2002). Crystalline structure of bleached and unbleached wheat straw (Triticum aestivum L.) soda-oxygen pulp. *Turk. J. Agric. For*., **26**, 247-252.

Gumuskaya, E., Usta, M., Kirci, H. (2003). The effects of various pulping conditions on crystalline structure of cellulose in cotton linters. *Polymer Degradation and Stability*, **81**, 559-564.

Hult L E, Iversen T, Sugiyama J. (2003). Characterization of the supramolecular structure of cellulose in wood pulp fibres. *Cellulose*, **10**:103-110.

Lindedahl K. (2008). Chemical reaction in Kraft Pulping. [Online] Available: http://www.h2obykl.com/images/Reactions%20in%20Kraft%20Pulping.pdf.

Lionetto F., Del Sole R., Cannoletta D., Vasapollo G., Maffezzoli A. (2012). Monitoring wood degradation

during weathering by cellulose crystallinity. *Materials*, **5**, 1910-1922. doi:10.3390/ma5101910.

Mann J. (1962). Modern methods of determining crystallinity in cellulose. *Pure. Appl. Chem*. **5**, 91-105.

Nishiyama Y., Kuga S., Okano T. (2000). Mechanism of mercerization revelead by x ray diffraction. *J. Wood. Sci.* **46**, 452-457.

Oh S.Y., Yoo D.I., Shin Y., Kim H.C., Kim H.Y., Chung Y.S., Park W.H., Youk J.H. 2005. Crystalline structure analysis of cellulose treated with sodium hydroxide and carbon dioxide by means of X-Ray diffraction and FT-IR spectroscopy. *Carbohyd Res*, **340**, 2376-2391.

Ouidiani A.E., Chaabouni Y., Msahli S., Sakli F. (2011). Crystal transition from cellulose I to cellulose II in NaOH treated Agave americana L. fibre. *Carbohydrate Polymers*, **86**, 1221-1229.

Owen N.L, Thomas D.W. (1989). Infrared studies of "hard" and "soft" woods. Appl. *Spectroscopy*, **43**, 451–455.

Park S., Baker J.O., Himmel M.E., Parilla P.A., Johnson D.K. (2010). Cellulose crystallinity index: measurement techniques and their impact on interpreting cellulase performance. *Biotechnology for Biofuels*, 3:10. [Online] Available: http://www.biotechnologyforbiofuels.com/content/3/1/10.

Potucek F., Milichovsky M. (2000). "Kraft pulp bleaching with hydrogen peroxide and peracetic acid. *Chems. Papers* **54**(6a), 406-411. Presented at the 27th International Conference of the Slovak Society of Chemical Engineering, Tatranske Matliare, 22-26 May 2000.

Segal L., Creely J.J., Jr. Martin A.E., Conrad C.M. (1962). An empirical method for estimating the degree of crystallinity of native cellulose using X-ray diffractometer. *Tex. Res. J*., **29**, 786-794.

Shatalov AA, Pereira H. (2005). *Bioresource Technology*, **96** (8), 865

Tashiro, K., Kobayashi, M. (1990). Theoritical evaluation of three-dimensional elastic constants of native and regenerated celluloses: role of hydrogen bonds. *Polymers*, **32**(8), 1516-1526.

Terinte N., Ibbett R., Schuster K.C. (2011). Overview on native cellulose and microcrystalline cellulose I structure studied by x-ray diffraction (WAXD): Comparison between measurement techniques. *Lenzinger Berichte*, **89**, 118-131.

Thygesen A, Oddershede J, Lilholt H, Thomsen AB, Stahl K. (2005). On the determination of crystallinity and cellulose content in plant fibres. *Cellulose*, **12**:563-576.

Wada, M., Okano, T., Sugiyama, J. (2001). Allomorphs of native crystalline cellulose I evaluated by two equatorial d-spacings. *J Wood Sci*, **47**, 124-128.

Zaibo, H., Kwak, Zhang, Z.C., Brown, H.M., Arey, B.W., Holladay, J.E. (2007). Studying cellulose fibers structure by SEM, XRD, NMR and acid hydrolysis. *Carbohydrate Polymers*, **68**, 235-241.

Ziaie-Shirkolaee Y. (2009). Comparative study on hydrogen peroxide bleaching of soda-organosolv and kraft rice straw pulps. *Indian Journal of Chemical Technology*, **16**, 181-187.

Zugenmaier P. (2001). Conformation and Packing of various crystalline cellulose fibers. *Prog. Polym. Sci*. **26**, 1341-1417.

The IISTE is a pioneer in the Open-Access hosting service and academic event management. The aim of the firm is Accelerating Global Knowledge Sharing.

More information about the firm can be found on the homepage:
http://www.iiste.org

CALL FOR JOURNAL PAPERS

There are more than 30 peer-reviewed academic journals hosted under the hosting platform.

Prospective authors of journals can find the submission instruction on the following page: http://www.iiste.org/journals/ All the journals articles are available online to the readers all over the world without financial, legal, or technical barriers other than those inseparable from gaining access to the internet itself. Paper version of the journals is also available upon request of readers and authors.

MORE RESOURCES

Book publication information: http://www.iiste.org/book/

Academic conference: http://www.iiste.org/conference/upcoming-conferences-call-for-paper/

IISTE Knowledge Sharing Partners

EBSCO, Index Copernicus, Ulrich's Periodicals Directory, JournalTOCS, PKP Open Archives Harvester, Bielefeld Academic Search Engine, Elektronische Zeitschriftenbibliothek EZB, Open J-Gate, OCLC WorldCat, Universe Digtial Library , NewJour, Google Scholar